Structural Studies of the Novel Antitumor Agents 4-Amino- and 4-Methoxy-8-(β-D-ribofuranosylamino)pyrimido[5,4-*d*]pyrimidines and Their α-Anomers Using X-ray, ^{1}H NMR, and Theoretical Methods

Arup K. Ghose,* Yogesh S. Sanghvi, Steven B. Larson,* Ganapathi R. Revankar, and Roland K. Robins

Contribution from the ICN Nucleic Acid Research Institute, 3300 Hyland Avenue, Costa Mesa, California 92626. *Received July 3, 1989*

Abstract: The structural properties of the new antitumor agents 4-amino- (ARPP, **1a**) and 4-methoxy-8-(β-D-ribofuranosylamino)pyrimido[5,4-*d*]pyrimidines (MRPP, **1b**) and the corresponding α-anomers **2a** and **2b** were studied by using molecular mechanics, molecular orbital (AM1) calculations, X-ray diffraction, and ^{1}H NMR spectral data. In the ^{1}H NMR spectra of **1a** and **1b** at elevated temperature, substantial upfield shifts for the exocyclic N*H* proton resonance were observed as compared to the spectra of the α-anomers. The crystal structures of MRPP ($C_{12}H_{15}N_5O_5\cdot H_2O$, **1b**) and its α-anomer ($C_{12}H_{15}N_5O_5\cdot H_2O$, **2b**) have been determined by single-crystal X-ray diffraction techniques employing Cu Kα radiation. Nucleoside **1b** crystallized in the monoclinic space group *C*2 with cell dimensions a = 13.309 (3) Å, b = 8.211 (2) Å, c = 14.025 (5) Å, β = 112.37 (3)°, and Z = 4. The structure was refined to a conventional R value of 0.0346 for 2369 reflections ($F \geq 4\sigma_F$). The α-anomer **2b** crystallized in the monoclinic space group *I*2 with cell dimensions a = 14.543 (2) Å, b = 4.7405 (13) Å, c = 21.355 (7) Å, β = 95.041 (14)°, and Z = 4 and was refined to R = 0.0338 for 2524 reflections ($F \geq 4\sigma_F$). The sugar conformations and puckering parameters are $^3T_2$ (C3′-endo/C2′-exo), P = −1.3°, and τ_m = 36.5° for **1b** and $_2T^3$ (C2′-exo/C3′-endo), P = 0.6°, and τ_m = 38.9° for **2b**. The dihedral angles between the fused pyrimidine rings are 2.55 (10)° for **1b** and 1.09 (9)° for **2b**. In each structure (**1b** and **2b**), all hydroxyl and amino hydrogen atoms are involved in intermolecular hydrogen bonding; no intramolecular hydrogen bonding is observed. The ^{1}H NMR spectrum of 5′-deoxy-MRPP (**3d**) also exhibited an upfield shift for the exocyclic N*H* proton signal at elevated temperature. An analysis of the molecular mechanics and molecular orbital conformational results together with X-ray crystallography and ^{1}H NMR data indicates that the reversible upfield shift shown by the exocyclic N*H* proton of these β-nucleosides is a conformational property rather than an effect of intramolecular hydrogen bonding.

We recently reported the synthesis and antitumor activity of several exocyclic aminonucleosides,[1-5] including 4-substituted 8-(D-ribofuranosylamino)pyrimido[5,4-*d*]pyrimidines[1] (**1**, **2**). Among these nucleosides, 8-(D-ribofuranosylamino) derivatives of 4-aminopyrimido[5,4-*d*]pyrimidine [ARPP, both β- (**1a**) and α- (**2a**) anomers] and 4-methoxypyrimido[5,4-*d*]pyrimidine (β-MRPP, **1b**) have shown promising antitumor activity against L1210, WI-L2, and LoVo/L cells in culture and against L1210 in mice.[1,5] The antitumor activity displayed by these nucleosides results from a sequence of enzyme interactions. First, the nucleosides are phosphorylated by adenosine kinase; second, the monophosphate thus formed inhibits PRPP synthetase. Although these nucleosides do not structurally resemble adenosine, they do act as substrates for adenosine kinase. Using our molecular modeling software REMOTEDISC,[7] we recently showed that these nucleosides, in some of their low-energy conformations, do resemble adenosine, thereby mimicking adenosine in adenosine kinase activity.[8] The observed antitumor activity[1] and the interesting molecular modeling studies[8] warranted a detailed structural study of these unusual nucleosides.

The ^{1}H NMR spectra of these compounds showed that the exocyclic N*H* proton resonates at lower field in the β-anomers (**1**) compared to the α-anomers (**2**). The study of the temperature dependence of this proton signal in **1** and **2** also revealed that it resonates at increasingly higher field, in the β-anomer only, as the temperature is increased. Such effects could be attributed to intramolecular hydrogen bonding. Furthermore, this interpretation is supported by the fact that two 2′,3′-*O*-isopropylidene derivatives of β-ARPP and β-MRPP exhibit N*H*···O5′ intramolecular hydrogen bonding in the solid state.[9] The crystal structure of ARPP (**1a**) has been reported by Narayanan and Berman.[10] Although no N*H*···O5′ intramolecular hydrogen bonding was observed, the conformation of the sugar ring is highly strained.[11] To resolve the ambiguity of the strained conformation of **1a** and the possibility of intramolecular hydrogen bonding, we have analyzed the ^{1}H NMR data of **1** and **2** in Me_2SO-d_6, studied the conformational properties by using molecular mechanics and AMPAC (AM1) molecular orbital methods, and correlated the data with single-crystal X-ray diffraction studies. We also synthesized 4-methoxy-8-[(5-deoxy-β-D-ribofuranosyl)amino]pyrimido[5,4-*d*]pyrimidine (**3d**) as a reference compound in which the possibility of N*H*···O5′ hydrogen bonding does not exist.

Experimental Section

Chemistry. The nucleosides **1** and **2** were synthesized and reported previously from our laboratory.[1] Compound **3d** was prepared as described below.

(1) Sanghvi, Y. S.; Larson, S. B.; Matsumoto, S. S.; Nord, L. D.; Smee, D. F.; Willis, R. C.; Avery, T. L.; Robins, R. K.; Revankar, G. R. *J. Med. Chem.* **1989**, *32*, 629.
(2) Moss, R. J.; Petrie, C. R.; Meyer, R. B., Jr.; Nord, L. D.; Willis, R. C.; Smith, R. A.; Larson, S. B.; Kini, G. D.; Robins, R. K. *J. Med. Chem.* **1988**, *31*, 786.
(3) Sanghvi, Y. S.; Larson, S. B.; Robins, R. K.; Revankar, G. R.; Gupta, P. K.; George, R. D.; Dalley, N. K. *J. Heterocycl. Chem.* **1988**, *25*, 623.
(4) Berman, H. M.; Rousseau, R. J.; Mancuso, R. W.; Kreishman, G. P.; Robins, R. K. *Tetrahedron Lett.* **1973**, *14*, 3099.
(5) Westover, J. D.; Revankar, G. R.; Robins, R. K.; Madsen, R. D.; Ogden, J. R.; North, J. A.; Mancuso, R. W.; Rousseau, R. J.; Stephan, E. L. *J. Med. Chem.* **1981**, *24*, 941.
(6) (a) Willis, R. C.; Nord, L. D.; Fujitaki, J. M.; Robins, R. K. *Adv. Enzyme Regul.* **1989**, *28*, 167. (b) Nord, L. D.; Willis, R. C.; Breen, T. S.; Avery, T. L.; Finch, R. A.; Sanghvi, Y. S.; Revankar, G. R.; Robins, R. K. *Biochem. Pharmacol.* **1989**, *38*, 3543.
(7) Ghose, A. K.; Crippen, G. M.; Revankar, G. R.; Smee, D. F.; McKernan, P. A.; Robins, R. K. *J. Med. Chem.* **1989**, *32*, 746.
(8) Ghose, A. K.; Viswanadhan, V. N.; Sanghvi, Y. S.; Nord. L. D.; Willis, R. C.; Revankar, G. R.; Robins, R. K. *Proc. Natl. Acad. Sci. U.S.A.* **1989**, *86*, 8242.
(9) Larson, S. B.; Sanghvi, Y. S.; Revankar, G. R.; Robins, R. K. *Acta Crystallogr.* **1989**, *C45*, 1194.
(10) Narayanan, P.; Berman, H. M. *Carbohydr. Res.* **1975**, *44*, 169.
(11) Altona, C. A.; Sundaralingam, M. *J. Am. Chem. Soc.* **1972**, *94*, 8205.

0002-7863/90/1512-3622$02.50/0

4-Methoxy-8-[(5-deoxy-β-D-ribofuranosyl)amino]pyrimido[5,4-*d*]pyrimidine (3d). Rydon reagent[12] (3 g, 6.56 mmol) was added to a solution of 4-methoxy-8-[(2,3-*O*-isopropylidene-β-D-ribofuranosyl)amino]-2,6-dichloropyrimido[5,4-*d*]pyrimidine[1] (**3a**, 2.2 g, 5.26 mmol) in dry DMF (60 mL) under an argon atmosphere, and the resultant solution was stirred for 1 h at room temperature with the exclusion of moisture. Methanol (1 mL) was added and the reaction mixture stirred for an additional 10 min. The solvent was removed under reduced pressure and the residue dissolved in EtOAc (150 mL). The organic phase was washed with 1 N $Na_2S_2O_3$ solution (100 mL), followed by water (100 mL), and dried over anhydrous Na_2SO_4. The solvent was evaporated, and the residual crude 4-methoxy-8-[(5-deoxy-5-iodo-2,3-*O*-isopropylidene-β-D-ribofuranosyl)amino]-2,6-dichloropyrimido[5,4-*d*]pyrimidine (**3b**) was hydrogenated by using Pd/C (10%, 1 g) and NaOAc (1.31 g, 16 mmol) in MeOH (100 mL) at 50 psi in a Parr hydrogenator for 24 h. The catalyst was removed by filtration through a Celite pad and washed with MeOH (2 × 50 mL). The combined filtrates were evaporated, and the residue was purified on a silica gel column (2.5 × 40 cm) with hexanes/EtOAc (7:3 v/v) as the eluent to provide 0.59 g of 4-methoxy-8-[(5-deoxy-2,3-*O*-isopropylidene-β-D-ribofuranosyl)amino]pyrimido[5,4-*d*]pyrimidine (**3c**): mp 65 °C (foams); ^{1}H NMR ($CDCl_3$) δ 1.34 (s, 3 H, C*H*$_3$), 1.37 (d, 3 H, *J* = 6 Hz, C5′*H*$_3$), 1.58 (s, 3 H, C*H*$_3$), 4.23 (s, 3 H, OC*H*$_3$), 4.27 (m, 1 H, C4′*H*), 4.51 (m, 1 H, C3′*H*), 4.83 (m, 1 H, C2′*H*), 5.91 (d of d, 1 H, C1′*H*), 7.30 (d, 1 H, *J* = 10 Hz, N*H*), 8.68 and 8.75 (2 s, 2 H, C2*H* and C6*H*). In the final deisopropylidenation step, compound **3c** (0.50 g) was stirred in a mixture of trifluoroacetic acid/H_2O (3 mL; 9:1 v/v) at room temperature for 30 min. The mixture was diluted with water (25 mL) and evaporated with EtOH (3 × 50 mL), followed by toluene (50 mL). The white residue was suspended in acetone (5 mL), warmed to dissolve, and cooled to furnish 0.30 g of the title compound **3d**: mp 198 °C dec; UV λ_{max} nm ($\epsilon \times 10^{-3}$) at pH 1, 299 (16.8), 310 (19.9), and 324 (14.0), at pH 7, 283 (13.4), 297 (sh, 11.9), 309 (11.8), and 324 (8.1), at pH 11, 283 (13.5), 297 (sh, 11.9), 309 (11.8), and 325 (8.1): ^{1}H NMR (Me_2SO-d_6) δ 1.19 (d, 3 H, *J* = 6 Hz, C5′*H*$_3$), 3.75 (m, 2 H, C3′*H* and C4′*H*), 4.11 (s, 3 H, OC*H*$_3$), 4.27 (m, 1 H, C2′*H*), 4.90 and 5.05 (2 d, 2 H, C2′O*H* and C3′O*H*), 5.77 (d of d, 1 H, C1′*H*), 8.59 and 8.83 (2 s, 2 H, C2*H* and C6*H*), 8.93 (d, 1 H, *J* = 9.3 Hz, N*H*). Anal. Calcd for $C_{12}H_{15}N_5O_4$: C, 49.14; H, 5.15; N, 23.88. Found: C, 48.99; H, 4.90; N, 23.64.

Single-Crystal X-ray Diffraction Studies. 4-Methoxy-8-[(β-D-ribofuranosyl)amino]pyrimido[5,4-*d*]pyrimidine (MRPP, **1b**) and its α-anomer (**2b**) were crystallized from a $CHCl_3$/MeOH solution by slow evaporation; crystals of **1b** grew as very thin plates and crystals of **2b** grew as needles. Table I summarizes data collection and refinement of **1b** and **2b**.

Initial models containing all non-hydrogen atoms including the water of solvation were obtained for both structures with the direct methods program SHELXS86;[13] all hydrogen atom positions were obtained from difference maps (**1b**, peaks of 0.32–0.89 e/Å^3 at *R* = 0.056; **2b**, peaks of 0.29–0.82 e/Å^3 at *R* = 0.059). Refinement of all possible parameters (anisotropic treatment of non-hydrogen atoms and isotropic treatment of hydrogen atoms) for each structure was accomplished with the full-matrix least-squares refinement program SHELX76.[14] Scattering factors and anomalous-dispersion corrections for non-hydrogen atoms were taken from *International Tables for X-ray Crystallography*,[15] and those for hydrogen atoms were from Stewart et al.[16] Data reduction was effected with the SDP-Plus system;[17] Figures 2–4 were drawn with ORTEPII.[18] Least-squares planes were calculated with the program PLANES.[19]

^{1}H NMR Study. (i) Temperature-dependent spectra: Proton nuclear magnetic resonance (^{1}H NMR) spectra were recorded in Me_2SO-d_6 at 300 MHz with an IBM NR/300 spectrometer. The chemical shift values are expressed in δ values (parts per million) relative to tetramethylsilane as an internal standard. The signals are described as s (singlet), d (doublet), t (triplet), q (quartet), and m (multiplet). For the temperature-dependent spectral studies, the spectra were recorded at intervals of 10 °C. (ii) Calculation of coupling constants: Calculation of the vicinal H–H coupling constant in an ethane-like system from the H–C–C–H dihedral angle was first suggested by Karplus.[20] Although the original Karplus equation was derived strictly for ethane, subsequently it was reparametrized to apply to a specific class of compounds, like nucleotides[21] or peptides,[22] or to generalize the substituent effect.[23,24] Later, Remin[25,26] utilized Haasnoot's[24] equation to study the conformational

Table I. Crystallographic Summary for **1b** and **2b**

	1b	**2b**
	A. Crystal Data[a]	
formula	$C_{12}H_{15}N_5O_5 \cdot H_2O$	$C_{12}H_{15}N_5O_5 \cdot H_2O$
formula wt	327.30	327.30
crystal system	monoclinic	monoclinic
space group	*C*2	*I*2
a, Å	13.309 (3)	14.543 (2)
b, Å	8.211 (2)	4.7405 (13)
c, Å	14.025 (5)	21.355 (7)
β, deg	112.37 (3)	95.041 (14)
V, Å^3	1417.5 (7)	1466.5 (7)
Z	4	4
T, K	295	295
D_x, g cm^{-3}	1.534	1.482
F_{000}	688	688
μ (Cu Kα), cm^{-1}	10.187	9.846
	B. Data Collection[b]	
mode	ω–2θ scan	
scan range	0.80 + 0.15 tan θ	
background	scan 0.25 times scan range before and after scan	
scan rate, deg min^{-1}	2.1–16.5	2.1–16.5
2θ range, deg	3–152	3–152
exposure time, h	44.5	33.3
stability cor range on *I*	1.000–1.000	0.996–1.000
range in *hkl*, min	0,–10,–17	0,–5,–26
range in *hkl*, max	16,10,17	18,5,26
total reflcns measd, unique	3082, 2931	3144, 2979
R_{int}	0.021	0.018
crystal dimensions, mm	0.485 × 0.29 × 0.01	0.40 × 0.12 × 0.06
crystal vol, mm^3	0.00139	0.00281
crystal faces	{001}; (100); (3,$\bar{4}$,$\bar{1}$); (3,4,1); (5,1,$\bar{1}$); ($\bar{5}$,$\bar{1}$,1)	{101}; {010}; {001}
transmission factor range	0.688–0.990	0.584–0.945
	C. Structure Refinement[c]	
reflcns used, *m* ($F \geq 4\sigma_F$)	2369	2524
no. of variables, *n*	276	276
extinction parameter	3.7 (5) × 10^{-7}	8.5 (8) × 10^{-7}
goodness of fit, *S*	1.373	1.536
R, *wR*	0.0346, 0.0444	0.0338, 0.0487
R for all data	0.0607	0.0502
max, av Δ/σ	0.0015, 0.0003	0.0017, 0.0003
max, min ρ in ΔF map (e Å^{-3})	0.41, –0.30	0.30, –0.24

[a] Unit-cell parameters were obtained by least-squares refinement of the setting angles of 25 reflections with 47.0° < 2θ < 55.6° for **1b** and 51.4° < 2θ < 59.8° for **2b**. [b] Enraf-Nonius CAD4 diffractometer with a graphite monochromator was used. Data reduction, which included Lorentz, polarization, decay, and absorption corrections, was accomplished with SDP-Plus software (Frenz, 1985). Crystal and instrument stabilities were monitored by remeasurement of three check reflections [for **1b**, (1,1,7), (2,4,$\bar{2}$), and (7,$\bar{1}$,$\bar{3}$); for **2b**, (1,2,9), (3,2,$\bar{9}$), and (8,$\bar{1}$,$\bar{3}$)] every hour. A linear fit of the intensities of these reflections was used to correct the data. Absorption corrections were based on measurement of crystal faces to define the shape and size of the crystals used. [c] Function minimized was $\sum w(|F_o| - |F_c|)^2$, where $w^{-1} = (\sigma_F^2 + 0.0004F^2)$ for both structures. $R = \sum||F_o| - |F_c||/\sum|F_o|$; $wR = [\sum w(|F_o| - |F_c|)^2/\sum w|F_o|^2]^{1/2}$. $S = [\sum w(|F_o| - |F_c|)^2/(m - n)]^{1/2}$. $\sigma_F = F\sigma_I/2I$; $\sigma_I = [N_{pk} + N_{bg1} + N_{bg2}]^{1/2}$.

(12) Verheyden, J. P. H.; Moffatt, J. G. *J. Org. Chem.* **1970**, *35*, 2319.
(13) Sheldrick, G. M. *SHELXS86, A Crystallographic Computing Package*; University of Göttingen: Göttingen, Federal Republic of Germany, 1986.
(14) Sheldrick, G. M. *SHELX76, A Crystallographic Computing Package*; University of Cambridge: Cambridge, England, 1976.
(15) *International Tables for X-ray Crystallography*: Kynoch Press: Birmingham, England, 1974; Vol. 4 (present distributor Kluwer Academic Publishers: Dordrecht, The Netherlands).
(16) Stewart, R. F.; Davidson, E. R.; Simpson, W. T. *J. Chem. Phys.* **1965**, *42*, 3175.
(17) Frenz, B. A. *Enraf-Nonius SDP-Plus Structure Determination Package*, Version 3.0; Enraf-Nonius: Delft, The Netherlands, 1985.
(18) Johnson, C. K. ORTEPII: A Fortran Thermal-Ellipsoid Plot Program for Crystal Structure Illustrations, Third Revision. Report ORNL-5138; Oak Ridge National Laboratory: Oak Ridge, TN, March 1976.
(19) Cordes, A. W. Personal communication, 1983.
(20) Karplus, M. *J. Am. Chem. Soc.* **1963**, *85*, 2870.
(21) Altona, C. A.; Sundaralingam, M. *J. Am. Chem. Soc.* **1973**, *95*, 2333.
(22) Kopple, K. D.; Wiley, G. R.; Tauke, R. *Biopolymers* **1973**, *12*, 627.
(23) Abraham, R. J.; Pachler, K. G. R. *Mol. Phys.* **1964**, *7*, 165.
(24) Haasnoot, C. A. G.; De Leeuw, F. A. A. M.; Altona, C. *Tetrahedron* **1980**, *36*, 2783.
(25) Remin, M. *J. Biomol. Struct. Dyn.* **1984**, *2*, 211.
(26) Remin, M. *J. Biomol. Struct. Dyn.* **1988**, *6*, 367.

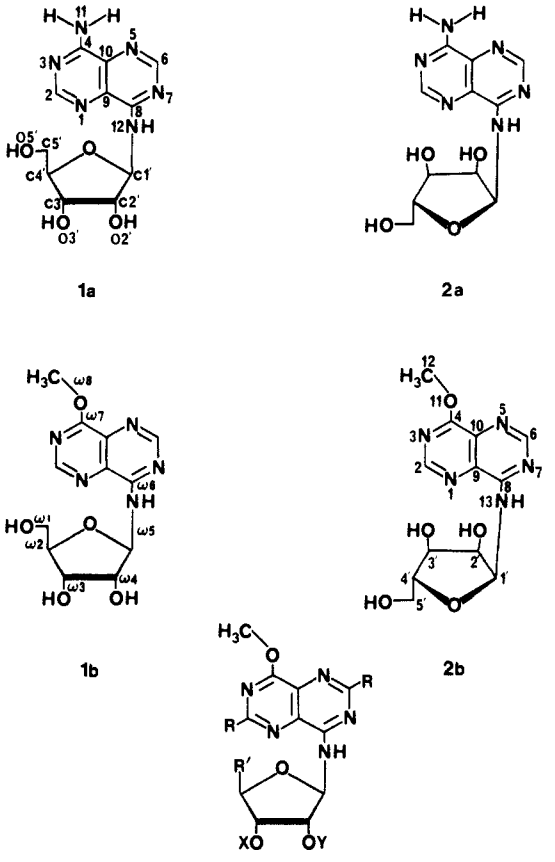

Figure 1. General structure, atom numbering, and identification of the dihedral angles of the compounds studied here.

properties of the nucleic acid components. In the present study we used Haasnoot's equation

$$J_{HH} = P_1 \cos^2 \phi + P_2 \cos \phi + P_3 + \sum \Delta\chi_i [P_4 + P_5 \cos^2 (\xi_i \phi + P_6 |\Delta\chi_i|)] \quad (1)$$

to evaluate the theoretical coupling constants in various conformations based on the H–C–C–H torsion angle ϕ. The effect of the group substituents was determined by the equation

$$\Delta\chi^{group} = \Delta\chi^{\alpha} - P_7 \sum \Delta\chi^{\beta} \quad (2)$$

where α is the atom directly attached to the ethane carbon and β are the atoms attached to the α atom. In eqs 1 and 2, the P's are the various parametrized constants,[24] $\Delta\chi_i$ is the difference in the electronegativity between the ith substituent and hydrogen, and ξ_i is the sign of the ith substituent. The parameters for the four substituted ethane-like system were used throughout this work.[24]

Molecular Mechanics (MM) Conformational Analysis. The fixed valence structure conformational analysis program CONFOR[27,28] was used for the conformational calculations. This program uses the 1985 MM2 parameters[29] with some additional torsional parameters obtained from the literature or from analogous bonds. The additional torsional parameters are given in the supplementary material.

Molecular Orbital (MO) Calculations. The AMPAC (AM1)[30,31] molecular orbital package was used for partial and complete geometry optimizations, starting from various conformations of interest, to evaluate the local minima.

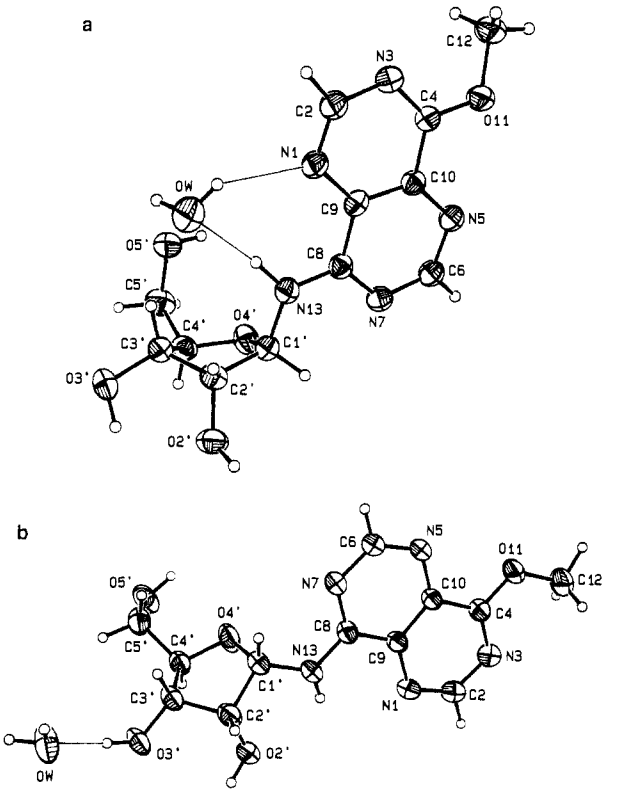

Figure 2. ORTEP drawings of molecules **1b** (a) and **2b** (b).

Results and Discussion

X-ray Study. The molecular conformations and atom labeling for compounds **1b** and **2b** are shown in Figure 2. The atomic coordinates are listed in Table II; bond lengths and bond angles are listed in Table III.

The Aglycon Moiety. As observed in ARPP (**1a**),[10] each of the two fused pyrimidine rings in each structure is essentially planar (rms deviation less than 0.020 Å for each ring); the dihedral angles between the planes are 2.55 (10)° for **1b** and 1.09 (9)° for **2b** compared to 0.59° for **1a**. The pyrimido[5,4-*d*]pyrimidine ring systems in **1b**, **2b**, and **1a** have bonding patterns of alternating long and short bonds with approximate 2-fold symmetry as diagrammed in Figure 1. The corresponding bond lengths and bond angles in **1b** and **2b** are equivalent within experimental error; the lengths of the bonds in **1a**, equivalent to bonds C4–C10 and C6–N7 in **1b** and **2b**, are significantly longer (1.455 and 1.376 Å, respectively). The methoxy group is slightly twisted out of the pyrimidopyrimidine plane [9.5 (2)° for **1b** and 3.02 (11)° for **2b**] with the methyl group trans to C10.

The Glycosyl Linkage. The C8–N13 bonds in **1b** and **2b** are conjugated with the heterocycle; these bonds are even shorter than those observed in **1a** [1.365 (4) Å]. However, the C1′–N13 glycosyl bonds in **1b** are about the same as those in **1a** [1.431 (4) Å]. In Table IV the torsion angles χ_{CN}, χ'_{CN}, and χ''_{CN} that characterize the conformation of the glycosyl bridge are given. The values are of approximately the same magnitude but opposite sign for **1b** and **2b**. Nucleosides **1b** and **1a** have torsion angles that are within 23° (rms deviation of χ, χ', and χ'' is ~19°) of each other.

The Glycon Moiety. Nucleoside **1b** was confirmed to be the β-anomer and **2b** was confirmed to be the α-anomer. The conformational parameters[11] of the ribose moieties are given in Table IV. The conformations in **1b** and **2b** are nearly identical despite the difference in anomeric configuration but are very distinct from the unusual ribose conformation found in **1a**.[10] Bond lengths and bond angles are not significantly different between the two anomers of MRPP. However, the orientations of the C5′–O5′ side chain do differ; the β-anomer has the gauche–gauche ($g+$) orientation

(27) Ghose, A. K.; Crippen, G. M. *J. Med. Chem.* **1984**, *27*, 901.
(28) Viswanadhan, V. N.; Ghose, A. K.; Revankar, G. R.; Robins, R. K. *J. Chem. Inf. Comput. Sci.* **1989**, *29*, 163.
(29) (a) QCPE Program No. 395; Department of Chemistry, Indiana University: Bloomington, IN. (b) N. L. Allinger, private communication, MMP2 1985 parameters, June 17, 1987.
(30) QCPE Program No. 506; Department of Chemistry, Indiana University: Bloomington, IN.
(31) Dewar, M. J. S.; Zoebisch, E. G.; Healy, E. F.; Stewart, J. J. P. *J. Am. Chem. Soc.* **1985**, *107*, 3902.

Table II. Positional and Equivalent Isotropic Thermal Parameters for All the Atoms in **1b** and **2b**

atom	*x/a*	*y/b*	*z/c*	U_{eq}[a]	atom	*x/a*	*y/b*	*z/c*	U_{eq}[a]
				1b					
N1	0.3139 (2)	0.7	0.38892 (14)	0.0351 (6)	O4′	0.35561 (12)	0.1966 (3)	0.22962 (11)	0.0398 (6)
C2	0.3416 (2)	0.8366 (4)	0.4407 (2)	0.0381 (8)	O5′	0.4504 (2)	0.4557 (3)	0.15131 (15)	0.0459 (7)
N3	0.3946 (2)	0.8558 (3)	0.5437 (2)	0.0367 (7)	OW	0.7025 (2)	0.1788 (4)	0.1637 (2)	0.0539 (8)
C4	0.4209 (2)	0.7225 (4)	0.5993 (2)	0.0312 (7)	H2	0.323 (2)	0.940 (4)	0.406 (2)	0.042 (7)
N5	0.4289 (2)	0.4268 (3)	0.61389 (14)	0.0347 (6)	H6	0.428 (2)	0.193 (4)	0.599 (2)	0.033 (6)
C6	0.4049 (2)	0.2903 (4)	0.5607 (2)	0.0364 (8)	H12A	0.553 (3)	0.931 (5)	0.707 (3)	0.070 (10)
N7	0.3534 (2)	0.2695 (3)	0.45801 (15)	0.0349 (6)	H12B	0.548 (3)	0.860 (5)	0.814 (3)	0.067 (10)
C8	0.3218 (2)	0.4024 (3)	0.3997 (2)	0.0299 (7)	H12C	0.441 (3)	0.960 (5)	0.729 (3)	0.065 (10)
C9	0.3429 (2)	0.5613 (4)	0.4474 (2)	0.0296 (6)	H13	0.259 (3)	0.488 (5)	0.257 (3)	0.073 (11)
C10	0.3966 (2)	0.5638 (4)	0.5542 (2)	0.0296 (6)	H1′	0.246 (2)	0.147 (4)	0.292 (2)	0.041 (7)
O11	0.47351 (14)	0.7299 (3)	0.70080 (12)	0.0408 (6)	H2′	0.109 (2)	0.306 (4)	0.131 (2)	0.039 (7)
C12	0.5108 (3)	0.8894 (4)	0.7426 (2)	0.0487 (10)	H3′	0.240 (2)	0.417 (4)	0.076 (2)	0.034 (6)
N13	0.2694 (2)	0.3889 (3)	0.29725 (14)	0.0358 (7)	H4′	0.336 (2)	0.099 (4)	0.096 (2)	0.046 (8)
C1′	0.2576 (2)	0.2349 (4)	0.2442 (2)	0.0342 (7)	H5′A	0.507 (3)	0.233 (4)	0.145 (2)	0.060 (9)
C2′	0.1675 (2)	0.2379 (4)	0.1367 (2)	0.0354 (7)	H5′B	0.426 (3)	0.301 (5)	0.038 (3)	0.059 (9)
C3′	0.2296 (2)	0.2919 (4)	0.0707 (2)	0.0346 (7)	HO2′	0.072 (3)	0.047 (5)	0.122 (3)	0.075 (11)
C4′	0.3392 (2)	0.2074 (4)	0.1222 (2)	0.0353 (7)	HO3′	0.131 (4)	0.156 (6)	−0.041 (3)	0.094 (14)
C5′	0.4354 (2)	0.2924 (4)	0.1121 (2)	0.0448 (9)	HO5′	0.482 (4)	0.449 (6)	0.215 (4)	0.10 (2)
O2′	0.1297 (2)	0.0773 (3)	0.10434 (14)	0.0494 (7)	HWA	0.739 (3)	0.209 (5)	0.126 (3)	0.075 (11)
O3′	0.1765 (2)	0.2495 (3)	−0.03554 (12)	0.0462 (6)	HWB	0.727 (3)	0.233 (5)	0.220 (3)	0.063 (10)
				2b					
N1	0.47038 (12)	0.75	0.29023 (8)	0.0410 (6)	O4′	0.27485 (10)	0.2955 (7)	0.43367 (7)	0.0583 (6)
C2	0.52748 (15)	0.9292 (8)	0.26761 (10)	0.0442 (7)	O5′	0.17254 (11)	0.4180 (7)	0.54350 (8)	0.0577 (6)
N3	0.61839 (12)	0.9700 (7)	0.28631 (8)	0.0428 (6)	OW	0.96978 (13)	0.5600 (7)	0.38828 (11)	0.0640 (7)
C4	0.65335 (13)	0.8127 (7)	0.33269 (9)	0.0364 (6)	H2	0.502 (2)	1.037 (6)	0.2320 (11)	0.040 (6)
N5	0.63689 (10)	0.4563 (6)	0.41329 (8)	0.0396 (5)	H6	0.605 (2)	0.165 (6)	0.4715 (12)	0.044 (7)
C6	0.57871 (14)	0.2781 (7)	0.43686 (10)	0.0431 (7)	H12A	0.865 (2)	0.990 (7)	0.3440 (13)	0.054 (8)
N7	0.48921 (11)	0.2351 (7)	0.41773 (9)	0.0431 (6)	H12B	0.777 (2)	1.226 (10)	0.320 (2)	0.074 (10)
C8	0.45274 (13)	0.3853 (7)	0.36936 (9)	0.0361 (6)	H12C	0.803 (2)	0.942 (8)	0.278 (2)	0.075 (10)
C9	0.50746 (13)	0.5892 (7)	0.33943 (9)	0.0343 (6)	H13	0.344 (2)	0.452 (7)	0.3210 (13)	0.050 (8)
C10	0.59946 (12)	0.6112 (7)	0.36385 (9)	0.0342 (6)	H1′	0.340 (2)	−0.025 (6)	0.3921 (12)	0.046 (7)
O11	0.74207 (9)	0.8292 (7)	0.35351 (7)	0.0453 (5)	H2′	0.225 (2)	−0.092 (7)	0.3090 (13)	0.054 (8)
C12	0.7990 (2)	1.0226 (8)	0.32129 (13)	0.0523 (8)	H3′	0.170 (2)	−0.165 (6)	0.4097 (11)	0.041 (6)
N13	0.36381 (11)	0.3446 (7)	0.34821 (9)	0.0410 (6)	H4′	0.145 (2)	0.431 (7)	0.4256 (13)	0.049 (7)
C1′	0.30518 (14)	0.1586 (7)	0.37922 (10)	0.0412 (7)	H5′A	0.203 (2)	0.015 (8)	0.5162 (15)	0.069 (9)
C2′	0.21765 (14)	0.0809 (7)	0.33791 (10)	0.0404 (6)	H5′B	0.094 (2)	0.106 (8)	0.5052 (14)	0.064 (9)
C3′	0.15199 (13)	0.0217 (7)	0.38828 (10)	0.0369 (6)	HO2′	0.139 (2)	0.280 (8)	0.2775 (14)	0.065 (9)
C4′	0.17834 (13)	0.2504 (7)	0.43700 (10)	0.0356 (6)	HO3′	0.024 (2)	−0.113 (9)	0.374 (2)	0.075 (10)
C5′	0.1604 (2)	0.1794 (8)	0.50346 (12)	0.0488 (7)	HO5′	0.235 (2)	0.433 (8)	0.5532 (14)	0.062 (8)
O2′	0.19005 (10)	0.3184 (6)	0.30054 (7)	0.0482 (5)	HWA	0.919 (3)	0.533 (8)	0.414 (2)	0.075 (10)
O3′	0.05776 (10)	0.0376 (6)	0.36482 (8)	0.0464 (5)	HWB	1.002 (3)	0.377 (13)	0.390 (2)	0.109 (15)

[a] For non-hydrogen atoms, U is $U_{eq} = {}^1/_3\sum_i\sum_j U_{ij}a_i^*a_j^*A_{ij}$, where A_{ij} is the dot product of the ith and jth direct-space unit-cell vectors.

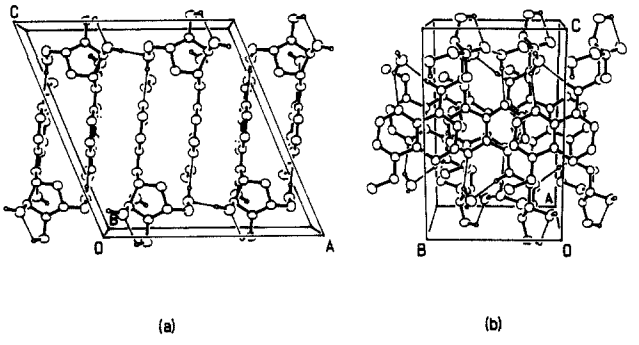

Figure 3. Crystal packing of **1b**. (a) View along the *b*-axis illustrating the base stacking. (b) View along the *a*-axis showing the nearly complete overlap of the bases.

and the α-anomer has the gauche–trans (*t*) orientation.

Packing. The hydrogen bonding in the two structures is detailed in Table V. It should be noted that the $-OCH_3$ group in **1b** has two hydrogen atoms in close contact with ribose oxygens. Nucleoside **1b** crystallizes with the pyrimido[5,4-*d*]pyrimidine base approximately parallel to the (2,0,−1) diffraction plane. However, base-stacking interactions occur mainly in a pairwise fashion as seen in Figure 3a. The nearly complete overlap of the bases in one of these hydrogen-bonded pairs is seen in Figure 3b. We have recently reported[32] the structure of 1-(2-deoxy-β-D-*erythro*-pentofuranosyl)-1*H*-pyrazolo[3,4-*b*]pyridin-4(7*H*)-one, which also exhibits pairwise, nearly complete base overlap as hydrogen-bonded dimers. In the present case the average interbase distance is 3.40 (3) Å, compared to 4 Å in the pyrazolo[3,4-*b*]pyridin-4(7*H*)-one. Atom O5′, which is involved in hydrogen bonding the pair together, is only −0.017 Å out of the plane of the base of the paired molecule.

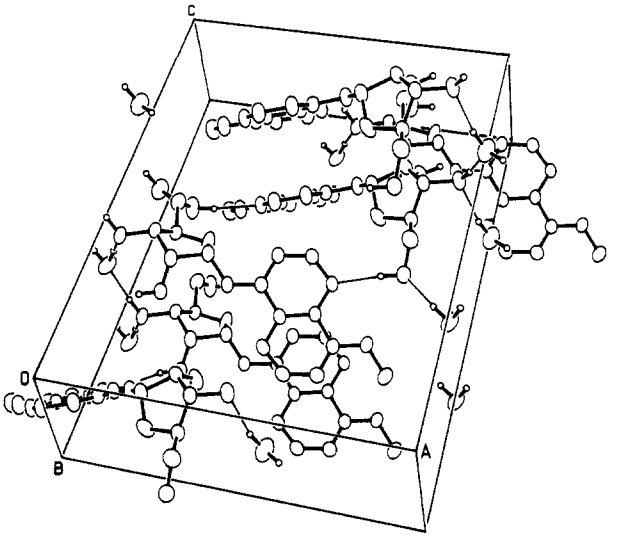

Figure 4. Packing diagram of **2b** viewed perpendicular to the pyrimido[5,4-*d*]pyrimidine ring of one molecule.

(32) Sanghvi, Y. S.; Larson, S. B.; Willis, R. C.; Robins, R. K.; Revankar, G. R. *J. Med. Chem.* **1989**, *32*, 945.

Table III. Bond Lengths (Å) and Bond Angles (deg) in **1b** and **2b**

1	2	3	1-2, **1b**	1-2, **2b**	1-2-3, **1b**	1-2-3, **2b**
C2	N1	C9	1.311 (3)	1.310 (3)	115.1 (2)	115.1 (2)
N3	C2	N1	1.353 (3)	1.361 (3)	127.8 (3)	128.0 (2)
C4	N3	C2	1.312 (4)	1.307 (3)	116.8 (3)	116.4 (2)
C10	C4	O11	1.431 (4)	1.436 (4)	117.0 (2)	115.9 (2)
C10	C4	N3			122.2 (2)	122.6 (2)
O11	C4	N3	1.327 (2)	1.330 (2)	120.8 (3)	121.4 (2)
C6	N5	C10	1.317 (4)	1.326 (4)	113.7 (2)	114.4 (2)
N7	C6	N5	1.350 (3)	1.345 (3)	128.8 (3)	127.9 (2)
C8	N7	C6	1.333 (3)	1.326 (3)	117.7 (2)	117.7 (2)
C9	C8	N13	1.443 (4)	1.437 (4)	120.1 (2)	120.0 (2)
C9	C8	N7			119.7 (2)	120.5 (2)
N13	C8	N7	1.342 (3)	1.346 (2)	120.2 (2)	119.4 (2)
C10	C9	N1	1.394 (3)	1.396 (2)	122.9 (2)	123.0 (2)
C10	C9	C8			116.2 (2)	115.7 (2)
N1	C9	C8	1.370 (3)	1.370 (3)	120.9 (2)	121.3 (2)
C4	C10	N5			120.8 (2)	121.4 (2)
C4	C10	C9			115.2 (2)	114.9 (2)
N5	C10	C9	1.369 (4)	1.360 (3)	123.9 (3)	123.7 (2)
C12	O11	C4	1.443 (4)	1.449 (4)	115.9 (2)	117.2 (2)
C1′	N13	C8	1.445 (4)	1.429 (4)	122.3 (2)	121.9 (2)
C2′	C1′	O4′	1.529 (3)	1.529 (3)	106.1 (2)	106.1 (2)
C2′	C1′	N13			112.6 (2)	112.4 (2)
O4′	C1′	N13	1.431 (3)	1.435 (3)	109.9 (2)	109.6 (3)
C3′	C2′	O2′	1.522 (4)	1.526 (3)	106.5 (2)	112.3 (2)
C3′	C2′	C1′			101.6 (2)	100.3 (2)
O2′	C2′	C1′	1.423 (4)	1.417 (4)	110.4 (2)	108.3 (2)
C4′	C3′	O3′	1.526 (3)	1.528 (4)	112.8 (2)	112.3 (2)
C4′	C3′	C2′			102.8 (2)	102.4 (2)
O3′	C3′	C2′	1.428 (3)	1.419 (2)	113.3 (2)	112.7 (2)
C5′	C4′	O4′	1.512 (4)	1.503 (3)	109.3 (2)	109.5 (2)
C5′	C4′	C3′			115.9 (2)	115.5 (3)
O4′	C4′	C3′	1.440 (3)	1.428 (2)	105.1 (2)	105.1 (2)
O5′	C5′	C4′	1.434 (4)	1.419 (4)	113.3 (3)	111.6 (3)
C1′	O4′	C4′			110.6 (2)	110.3 (2)

Table IV. Sugar Conformational Parameters in **1b**, **2b**, and **1a**

parameter		**1b**	**2b**	**1a**[a]
	Sugar Conformation			
τ_0, deg	C4′-O4′-C1′-C2′	11.5 (3)	13.7 (3)	-44.0
τ_1, deg	O4′-C1′-C2′-C3′	-30.1 (3)	-32.9 (3)	27.1
τ_2, deg	C1′-C2′-C3′-C4′	36.5 (3)	38.9 (3)	1.1
τ_3, deg	C2′-C3′-C4′-O4′	-30.7 (3)	-32.2 (3)	-25.4
τ_4, deg	C3′-C4′-O4′-C1′	12.1 (3)	11.7 (3)	43.9
τ_m, deg	amplitude of pucker[b]	36.5	38.9	45.0
P, deg	pseudorotation angle[b]	0.6	-1.3	88.6
	conformation	C3′-endo/ C2′-exo $^3T_2$	C2′-exo/ C3′-endo $_2T^3$	O4′-endo ^0E
	Glycosidic Linkage			
χ_{CN}, deg	O4′-C1′-N11-H11	82 (3)	-90 (3)	95 (7)
χ'_{CN}, deg	O4′-C1′-N11-C8	-79.8 (3)	78.5 (3)	-99.2 (5)
χ''_{CN}, deg	C1′-N11-C8-N7	-8.4 (4)	4.7 (4)	14.0 (7)
	Side-Chain Conformation			
ϕ_{OO}, deg	O4′-C4′-C5′-O5′	-61.2 (3)	71.2 (3)	-174.7
ϕ_{CO}, deg	C3′-C4′-C5′-O5′	57.2 (3)	-170.4 (2)	-58.3

[a] From ref 10. [b] See ref 11.

As in **1a**, there may be an intramolecular hydrogen-bonding interaction O3′ → O2′, although it is much weaker in **1b**, perhaps because it is bifurcated in an O3′ → O5′ interaction also. All OH and NH hydrogen atoms are involved in hydrogen bonding. The water molecule forms an unusual intramolecualr hydrogen-bonded bridge from N13 to N1 resulting in a seven-membered ring (Figure 2).

The hydrogen bonds existing in the crystal structure of **2b** are generally shorter and on the average more linear than those in the β-anomer. All OH groups act as donors. The hydrogen of the bridging NH is involved in an intramolecular interaction with O2′, having a geometry similar to the O3′ → O2′ interaction in **1b**. Bases stack along the *b* direction with an interplanar spacing of 3.33 Å. Partial overlap of one pyrimidine ring with the other pyrimidine ring of an adjacent molecule is observed. Heterocycles of 2-fold related molecules are approximately perpendicular to each other. These 2-fold related molecules again form dimers with reciprocated O5′ → N5 hydrogen bonds as in **1b**, but the heterocycles are perpendicular in **2b** rather than parallel as in **1b**.

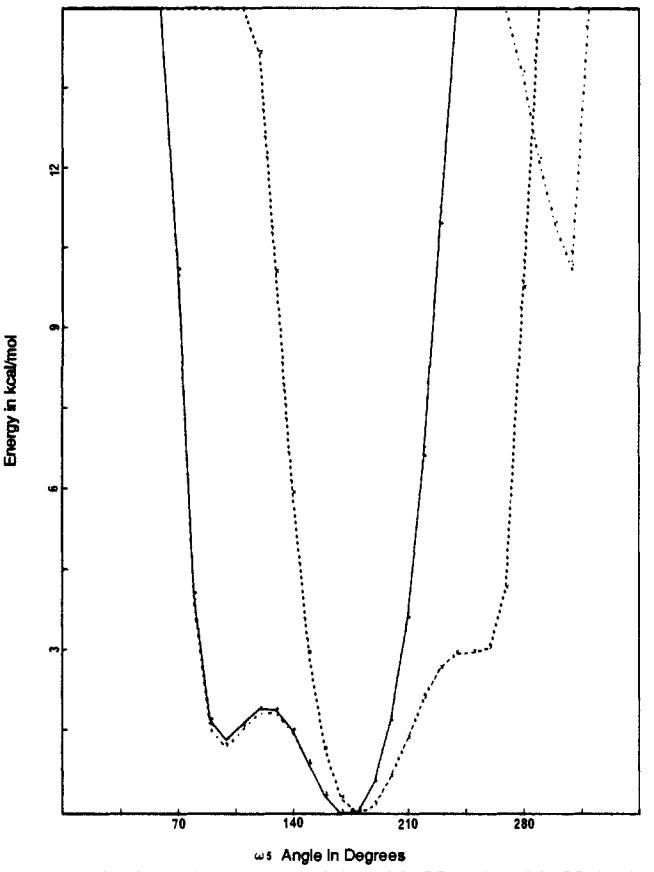

Figure 5. Conformational energy of the β-MRPP (—), α-MRPP (---), and 5′-deoxy-β-MRPP (·-·) during the rotation of the C1′-N (ω_5) bond. The rest of the dihedral angles were fixed at the values of their global minimum-energy conformation.

Molecular Mechanics Conformational Analysis. The initial valence structures of these molecules were generated from our crystallographic fragment library, containing the 2′-endo/3′-exo (type S) and 2′-exo/3′-endo (type N) ribose rings[33] and the pyrimido[5,4-*d*]pyrimidine rings.[9] The minimum energy conformations of **1** and **2**, as obtained from the pattern and combinatorial searches, are given in Table VI. During the pattern search minimization, all rotatable dihedral angles (see Table VI for identification of these angles) were rotated from 0° to 360° at intervals of 10°. For the combinatorial search only four dihedral angles (ω_1, ω_2, ω_5, and ω_6) were rotated; the latter three were rotated from 0° to 360° at intervals of 20°, while ω_1 was rotated from 60° to 300° at intervals of 120°. The β-anomers **1a** and **1b** showed remarkably similar conformational behavior. Not only were their minimum energy conformations almost identical (see Table VI), but also the energy profiles of the rotation of the two dihedral angles around the exocyclic N*H* were almost identical near the low-energy region. The MM calculations resulted in two significant observations: (1) in the β-anomer **1b** with regular S or N puckered ribofuranosyl moieties, O5′ and the exocyclic N*H* proton, even at their closest distance (3.63 and 3.20 Å, respectively), are too far apart to form a hydrogen bond; and (2) the β-anomers show two energy minima with respect to rotation about the C1′-N bond, whereas the α-anomers show only one minimum (see Figure 5).

^{1}H NMR Study and AM1 Molecular Orbital Calculations. The ^{1}H NMR spectra of the α- and β-anomers of ARPP and MRPP at 297 K exhibit considerable differences in the chemical shift of the N*H* protons ($\Delta\delta$ = 0.30 and 0.32 ppm, respectively). In each case, the N*H* signal of the β-anomer is downfield with respect

(33) Low, J. N. *Acta Crystallogr.* **1983**, *C39*, 796.

Table V. Hydrogen Bonding and Close Contacts in **1b** and **2b**

D	H	A	symmetry of A relative to D	*d* (D···A), Å	*d* (H···A), Å	∠ (D—H···A), deg
			1b			
C12	H12A	O4′	1.0 − *x*, 1.0 + *y*, 1.0 − *z*	3.026 (4)	2.49 (4)	116 (3)
C12	H12B	O3′	0.5 + *x*, 0.5 + *y*, 1.0 + *z*	3.262 (4)	2.34 (4)	161 (3)
N13	H13	OW	*x* − 0.5, 0.5 + *y*, *z*	2.950 (4)	1.99 (4)	168 (3)
O2′	HO2′	O5′	*x* − 0.5, *y* − 0.5, *z*	2.885 (3)	1.97 (4)	173 (4)
O3′	HO3′	O2′	*x*, *y*, *z*	2.678 (3)	2.15 (4)	113 (3)
O3′	HO3′	O5′	0.5 − *x*, *y* − 0.5, −*z*	3.038 (3)	2.23 (5)	140 (4)
O5′	HO5′	N5	1.0 − *x*, *y*, 1.0 − *z*	3.076 (3)	2.24 (5)	178 (5)
OW	HWA	O3′	1.0 − *x*, *y*, −*z*	2.892 (3)	2.02 (4)	173 (4)
OW	HWB	N1	0.5 + *x*, *y* − 0.5, *z*	2.940 (2)	2.22 (4)	141 (3)
			2b			
N13	H13	O2′	*x*, *y*, *z*	2.643 (2)	2.33 (3)	104 (2)
O2′	HO2′	N1	0.5 − *x*, *y* − 0.5, 0.5 − *z*	2.918 (2)	2.06 (3)	168 (3)
O3′	HO3′	OW	*x* − 1.0, *y* − 1.0, *z*	2.670 (3)	1.78 (4)	172 (4)
O5′	HO5′	N5	1.0 − *x*, *y*, 1.0 − *z*	2.849 (2)	1.95 (3)	171 (3)
OW	HWA	O5′	1.0 − *x*, *y*, 1.0 − *z*	2.719 (3)	1.77 (4)	170 (4)
OW	HWB	O3′	1.0 + *x*, *y*, *z*	2.852 (4)	1.90 (5)	161 (4)

Table VI. Minimum-Energy Conformation of the Molecules As Obtained from Molecular Mechanics Calculations[a]

	angle, deg							
compd	ω_1	ω_2	ω_3	ω_4	ω_5	ω_6	ω_7	ω_8
1a	50	60	50	290	170	160	340	
2a	50	60	50	290	180	170	340	
1b	50	60	50	290	170	160	10	60
2b	50	60	50	290	180	170	10	60
3d		60	50	290	170	190	100	60

[a] ω_1 = H–O5′–C5′–C4′, ω_2 = O5′–C5′–C4′–C3′, ω_3 = H–O3′–C3′–C2′, ω_4 = H–O2′–C2′–C1′, ω_5 = C2′–C1′–N12–C8 (for **1a** and **2a**) or C2′–C1′–N13–C8 (for **1b** and **2b**), ω_6 = H–N–C8–N7, ω_7 = N3–C4–N11–H(C) or N3–C4–O11–C, and ω_8 = C4–O11–C12–H. For atom labels, see Figure 1.

Table VII. AM1 Optimized Structures[a] of Nucleosides **1a**, **1b**, **2a**, and **2b**

	angle, deg							
compd	ω_1	ω_2	ω_3	ω_4	ω_5	ω_6	ω_7	ω_8
1a	72.9	76.2	65.9	−59.7	162.8	194.7	0.0	
2a	60.7	59.7	76.0	−58.4	201.3	163.9	−2.3	
1b	78.2	72.3	55.7	−57.6	167.6	193.5	−0.2	61.4
2b	60.1	61.2	84.5	−62.7	182.8	160.9	−0.2	179.9

[a] The starting structure in the optimization procedure was the molecular mechanics minimum-energy conformation as given in Table VI. For identification of the dihedral angles, see the footnote of Table VI.

to that of the α-anomer (8.40 vs 8.1 ppm in ARPP and 8.71 vs 8.39 ppm in MRPP). It has been shown by X-ray analysis,[1,9] and corroborated by low-field N*H* proton resonance,[1] that NH···O5′ intramolecular hydrogen bonding exists in the 2′,3′-*O*-isopropylidene-blocked precursors of **1**. Thus, it was postulated that NH···O5′ intramolecular hydrogen bonding was present in the deblocked β-anomers (**1**) studied here.[1]

To study this possibility, a variable-temperature ^{1}H NMR experiment (297 → 360 K) using Me_2SO-d_6[34] as solvent was initiated for nucleosides **1** and **2**. As the samples were heated and then cooled, compounds **1a** and **1b** exhibited a smooth and reversible shift of the N*H* resonance signal (**1a**, 8.40 ↔ 7.90 ppm; **1b**, 8.71 ↔ 8.17 ppm); the resonances of the N*H* protons of the α-anomers **2a** and **2b**, however, did not change in this temperature range. Except for the signals of the C4NH_2 protons in the ARPP anomers, all other proton signals remained relatively unaffected. The C4NH_2 signals appeared as two broad singlets at 297 K (**1a**, 7.77 and 7.92 ppm; **2a**, 7.78 and 8.0 ppm), indicating a difference in the environments of the two protons. At 360 K, both sets of signals collapsed to broad singlets (**1a**, 7.42 ppm; **2a**, 8.10 ppm). Since crystallographic evidence presented here and elsewhere[1,9,10] suggests that the N*H*···N1 spatial relationship is fairly constant (i.e., $\omega_6 \sim 180°$), these variable-temperature NMR studies corroborate the hypothesis that the low-field signal of the N*H* proton in the β-anomers **1** results from NH···O5′ hydrogen bonding.

However, the solid-state structures of **1a**[10] and **1b** (presented above) show no such hydrogen bonding. Furthermore, the MM studies of the structures, employing regular S or N puckered ribofuranosyl rings, suggest that the postulated hydrogen bonds are virtually impossible in the structures. Thus, in an effort to resolve this discrepancy, we did exhaustive AMPAC (AM1) MO calculations. The structures of **1** and **2**, obtained from the various crystallographic and MM energy minimization studies, were subjected to AM1 MO optimization to study their relative energies. Both partial and complete geometry optimizations were performed. The former, in which all non-hydrogen dihedral angles were fixed, resulted in a structure that was optimized with respect to bond distances and angles without change in conformation. The latter optimized the complete structure by varying all internal coordinates, resulting in optimized bond distances and angles and a change in conformation. Some of the important results of these studies are summarized in Tables VII and VIII.

When the dihedral angles ω_1 and ω_5 in both the S and N puckered structures of **1** were properly oriented to form an N*H*···O5′ hydrogen bond, the H···O distances were 3.63 and 3.20 Å, respectively. As shown in Table VIII, the complete geometry optimization decreased these distances considerably, placing these groups in a juxtaposition to form relatively weak hydrogen bonds. Other changes in these optimized structures involved the H1′–C1′–C2′–H2′ and H3′–C3′–C4′–H4′ dihedral angles as well as a flattening of the sugar rings. In terms of AMPAC (AM1) MO energy, the best structure was obtained from the geometry optimization of the MM minimum-energy conformation. The structure optimized from the crystal structure of **1b** presented above and the structure of **1a** generated from the crystal structure of the 2′,3′-*O*-isopropylidene-blocked nucleosides were energetically very close to the MM–MO-optimized structures. The energy of the structure of **1a** reported by Narayanan and Berman[10] had considerably higher energy. The partially optimized X-ray structure of **1a** had relatively high energy (−93.466 kcal/mol) and complete optimization resulted in a nearly planar furanose ring, having energy higher than the MM–MO geometry-optimized structure. Thus, the MO calculations demonstrate the tendency of the β-anomers to form the hydrogen bond if the sugar ring is flattened.

Therefore, we studied the sugar ring conformation, utilizing the H1′–H2′ and H3′–H4′ coupling constants after the manner of Remin.[25,26] The observed and calculated values of the coupling constants of the various conformations are given in Table IX. The calculated H1′–H2′ and H3′–H4′ coupling constants for the hydrogen-bonded conformations are generally very low and inconsistent with the observed coupling constants, whose values

(34) Our recent studies[8] show that nucleosides **1** and **2** anomerize rapidly in acidic solution and there was no change in **1** and **2** when ^{1}H NMR were recorded in Me_2SO-d_6.

Table VIII. Certain Aspects of the AM1 Molecular Orbital Calculation on Different Conformations of ARPP and MRPP

compd (source,[a] optimization[b])	energy, kcal/mol	important dihedral angles[c]				important distances	
		τ_1	τ_2	τ_3	τ_4	O5′–HN	N1–HN
1b (X, P)	−131.18	93.6	203.7	162.2	172.4	3.204	2.497
1b (X, C)	−134.47	101.6	223.2	161.2	164.1	2.503	2.485
1b (M, P)	−127.77	155.7	255.9	170.0	194.6	3.881	2.505
1b (M, C)	−134.97	119.9	247.3	167.6	162.2	2.450	2.476
1a (X, P)	−93.47	152.6	212.6	143.6	180.0	6.052	2.524
1a (X, C)	−98.81	130.4	231.9	140.6	163.5	4.925	2.472
1a (M, C)	−101.96	120.9	248.1	162.8	164.9	2.471	2.476
1a (X, C)[d]	−100.98	118.8	254.3	141.7	170.4	2.221	2.492
1a (X, C)[e]	−101.32	101.7	224.6	158.3	162.9	2.464	2.480
2b (X, C)	−130.64	−27.7	215.8	194.3	192.5	2.370[f]	2.500
2b (M, C)	−134.11	28.7	244.3	182.8	195.3	2.577[g]	2.498
2a (M, C)	−101.49	25.2	238.5	201.3	193.1	2.798[g]	2.493

[a] Source: X = X-ray; M = molecular mechanics. [b] Optimization: P = partial; C = complete. [c] τ_1 = H1′–C1′–C2′–H2′, τ_2 = H3′–C3′–C4′–H4′, τ_3 = C2′–C1′–N–C8, and τ_4 = C1′–N–C8–C9. [d] Generated from the X-ray crystal structure of the blocked nucleosides.[9] [e] Generated from the X-ray structure of β-MRPP. [f] O3′–H(N) distance. [g] O2′–H(N) distance.

Table IX. Observed and Calculated H1′–H2′ and H3′–H4′ Coupling Constants Using Karplus' Equation and Haasnoot's Modification[a]

compd[b]	$J_{1',2'}$ (K)	$J_{1',2'}$ (H)	$J_{1',2'}$ (O)	$J_{3',4'}$ (K)	$J_{3',4'}$ (H)	$J_{3',4'}$ (O)
1b (X, P)	−0.43	−0.44	5.66[c]	7.50	7.62	4.4[c]
1b (X, C)	−0.03	−0.36		4.64	3.61	
1b (M, P)	7.43	7.33	5.86[d]	0.16	−0.63	4.33[d]
1b (M, C)	1.99	1.21		1.03	−0.10	
1a (X, P)	7.04	6.80	5.80[c]	6.31	5.82	4.13[c]
1a (X, C)	3.60	2.81		3.24	1.98	
1a (M, C)	2.12	1.34	5.93[d]	0.94	−0.17	
1a (X, C)[e]	1.84	1.08		0.30	−0.57	
1a (X, C)[f]	−0.03	−0.36		4.43	3.34	
2b (X, C)	6.12	5.99	5.50[d]	5.83	5.14	4.35[c]
2b (M, C)	5.99	6.59		1.41	0.21	
2a (M, C)	6.42	7.00	5.43[d]	2.22	0.94	4.44[c]

[a] Column: K = Karplus,[20] H = Haasnoot,[24] and O = observed. [b] As in Table VIII. [c] Recorded in Me_2SO-d_6. [d] Recorded in Me_2SO-d_6 + D_2O. [e] See footnote *d* to Table VIII. [f] See footnote *e* to Table VIII.

correspond to an approximate S to N distribution of 60:40 for the conformations of the sugar rings. This evidence for normal S and N sugar puckering in compounds **1**, coupled with the MM studies and the solid-state structures, suggests that N*H*···O5′ hydrogen bonding is doubtful.

The above ambiguities led us to synthesize 5′-deoxy-MRPP {4-methoxy-8-[(5-deoxy-β-D-ribofuranosyl)amino]pyrimido[5,4-*d*]pyrimidine (**3d**)}, in which the possibility of N*H*···O5′ hydrogen bonding is eliminated by the absence of O5′. Following the standard deoxygenation procedure, 2,6-dichloro-4-methoxy-8-[(2,3-*O*-isopropylidene-β-D-ribofuranosyl)amino]pyrimido[5,4-*d*]pyrimidine (**3a**) was iodinated by using methyltriphenoxyphosphonium iodide[12] (Rydon reagent) in DMF to give **3b**, which was subsequently hydrogenated by using Pd/C to give **3c**. De-isopropylidenation of **3c** with TFA/H_2O provided **3d** as a crystalline product in 20% overall yield. The ^1H NMR of **3d** in Me_2SO-d_6 exhibited an N*H* chemical shift of 8.92 ppm at 297 K and 8.30 ppm at 360 K. This observation clearly demonstrated that the upfield shift of the N*H* proton resonance with increasing temperature in **1** was not due to intramolecular hydrogen bonding that had been postulated.

The upfield shift of the resonance of the exocyclic N*H* proton may be explained by conformational changes affecting the environment of the proton. Thus, we analyzed the conformational energies of the nucleosides **1**, **2**, and **3d** as a function of the dihedral angles about the C1′–N (ω_5) and N–C8 bonds (ω_6). During this analysis, all other dihedral angles were fixed at their global minimum-energy values. Only the rotation of ω_5 showed a considerable difference between the α- and β-anomers (see Figure 5). Each of the α-anomers **2a** and **2b** has a single energy minimum. The β-anomers **1** and **3d**, on the other hand, possess metastable local minima at $\omega_5 \sim 100°$, which represents a rotation about the C1′–N bond of 60–70° from the MO-optimized structures. Because the energy barrier separating these two minima is small, the corresponding conformations will be in equilibrium at all temperatures at which the ^1H NMR spectra were studied. However, due to the principle of mobile equilibrium,[35] the relative concentrations will change with temperature such that the population of the metastable conformation will increase with increasing temperature. This change in relative concentrations of the two conformations can explain the smooth reversible shift of this resonance of the exocyclic N*H* proton of the β-anomers.

Conclusion

The observed upfield shifts of 0.5–0.63 ppm for the resonances of the N*H* proton in **1** and **3d** over the temperature range 297 → 360 K are interpreted in terms of a conformational change about the C1′–N bond rather than the breaking of an intramolecular hydrogen bond. Although N*H*···O5′ hydrogen bonding has been observed in the crystal structures of some 2′,3′-*O*-isopropylidene-blocked nucleosides,[1,9] neither of the deblocked nucleosides (**1a** and **1b**) showed such hydrogen bonding. The MM calculations showed that H-bonding is not possible for regular S or N puckered ribofuranosyl conformations. The H1′–H2′ and H3′–H4′ coupling constants suggest S and N pucker in these nucleosides.

The solid-state molecular conformation of ARPP (**1a**), as reported by Narayanan and Berman,[10] has very high energy. The solid-state conformations of **1b** and **2b** reported in this study are very similar in energy and very close to the lowest energy conformations obtained from the MM and MO optimizations. There is, however, one significant difference between the α- and β-anomers in the rotational properties of the C1′–N bond. The α-anomers have only one energy minimum, whereas the β-anomers have two energetically close minima. The reversible upfield shift of the exocyclic amino proton resonance may be due to a change in the equilibrium between these two conformations.

In all the experimentally determined and theoretically calculated structures, we find one common feature of the bridging amine relative to the heterocyclic ring. The exocyclic N*H* proton is eclipsed to the N1 nitrogen of the heterocycle. Such an arrangement forms a quasi-five-membered ring, thereby creating a resemblance with adenosine.[8] Such a resemblance may also be created in a system like 5-fluoro-4-(β-D-ribofuranosylamino)pyrimidine and related compounds and may be the basis for the future synthesis of biologically active compounds related to purine nucleosides.

Supplementary Material Available: Tables of anisotropic thermal parameters, bond lengths and angles involving H atoms, torsion angles, and least-squares planes and a list of additional torsional parameters used in the CONFOR program (9 pages); structure factor amplitudes for both structures **1b** and **2b** (14 pages). Ordering information is given on any current masthead page.

(35) Glasstone, S. *Text Book of Physical Chemistry*; MacMillan: London, 1946; p 828.